Decoding ceRNA Regulatory Network in Pulmonary Artery of Hypoxia-Induced Pulmonary Hypertension (HPH) Rat Model

Jun Wang
Shenzhen University https://orcid.org/0000-0002-5470-4631
Yanqin Niu
Shenzhen University
Lingjie Luo
Shenzhen University
Zefeng Lu
Shenzhen University
Qinghua Chen
Shenzhen University
Shasha Zhang
Shenzhen University
Qianwen Guo
Shenzhen University
Li Li
Shenzhen University
Deming Gou (dmgou@szu.edu.cn)
Shenzhen University

Research

Keywords: HPH, ceRNA regulatory network, Differentially expressed RNAs, Diagnosis of PAH

Posted Date: October 26th, 2021

DOI: https://doi.org/10.21203/rs.3.rs-999962/v1

Version of Record: A version of this preprint was published at Cell & Bioscience on March 7th, 2022.
See the published version at https://doi.org/10.1186/s13578-022-00762-1.

Abstract

Background

Hypoxia-induced pulmonary hypertension (HPH) is a lethal cardiovascular disease with the characteristic of severe remodelling of pulmonary vascular. Although large number of dysregulated mRNAs, lncRNAs, circRNAs and miRNAs related to HPH have been identified in extensive studies, the RNA regulatory network in pulmonary artery that respond to hypoxia remains poorly understood.

Results

Transcriptomic profiles in pulmonary arteries of HPH rats were interrogated through high-throughput RNA sequencing in this study. The differentially expressed RNAs (DERNAs) including DEmRNAs, DElncRNAs, DEcircRNAs and DEmiRNAs between HPH and normal rats were investigated. A set of 19 DEmRNAs, 8 DElncRNAs, 19 DEcircRNAs and 23 DEmiRNAs were identified through a relatively strict screening. The DEmRNAs were further found to be involved in cell adhesion, axon guidance, PPAR signalling pathway and calcium signalling pathway, suggesting their crucial role in HPH. Furthermore, according to the competitive endogenous RNA (ceRNA) hypothesis, a hypoxia induced ceRNA regulatory network in pulmonary arteries of HPH rats was constructed. More specifically, the ceRNA network was composed of 10 miRNAs as hub nodes, which might be sponged by 6 circRNAs and 7 lncRNAs, and directed the expression of 18 downstream target genes that might play important role in the progression of HPH. Expression pattern of selected DERNAs in the ceRNA network were validated to be in consistent with sequencing results. Diagnostic effectiveness of several hub mRNAs were further evaluated through investigating their expression profiles in patients with pulmonary artery hypertension (PAH) recorded in the Gene Expression Omnibus (GEO) dataset GSE117261. Dysregulated POSTN, LTBP2, SPP1 and LSAMP were observed in both the pulmonary arteries of HPH rats and lung tissues of PAH patients.

Conclusions

A ceRNA regulatory network in pulmonary arteries of HPH rats was constructed, 10 hub miRNAs and their corresponding interacting lncRNAs, circRNAs and mRNAs were identified. The expression pattern of selected DERNAs were further validated to be in consistent with sequencing result. POSTN, LTBP2, SPP1 and LSAMP were suggested to be potential diagnostic biomarkers and therapeutic targets for PAH.

Background

Chronic hypoxia-induced pulmonary hypertension (HPH) is one of the most devasting cardiovascular disease that characterized by remodelling of vascular and elevation of pulmonary arterial pressure [1]. Increased right heart load is also another main characteristic of HPH, which may further lead to disturbance of pulmonary circulatory, right heart failure and ultimately death [2]. Although great

breakthrough has been made in illuminating the pathogenesis, identifying prognostic biomarkers and improving therapeutic strategies of HPH, the overall incidence and mortality rates remain high [3, 4]. Therefore, unveiling new insights into the development mechanisms of HPH is of great significance in facilitating further understanding of HPH.

A large number of RNAs participating in HPH development have been characterized in several previous studies [5, 6]. The RNA-mediated regulatory network consisting of both coding mRNAs and noncoding RNAs (lncRNAs, circRNAs and miRNAs) plays important role on the outcome of HPH. Dysregulated mRNAs that contributed to vascular remodelling, which is mainly due to excessive proliferation and migration of pulmonary artery smooth muscle cells (PASMCs), have been extensively reported [7–13]. These mRNAs were implicated in TGF-β signalling [7], Notch signalling [9], PI3K/AKT/mTOR signalling [8], PPAR signalling pathway [12, 13] and so on. Recent studies have also revealed that noncoding RNAs including lncRNAs, circRNAs and miRNAs were essential in mediating HPH pathogenesis as well [14–23]. For instance, lncRNA-MEG3 was proved to be upregulated in the cytoplasm of hypoxic PASMCs, which degraded the cytoplasmic miR-328-3p, and subsequently led to the upregulation of insulin-like growth factor receptor (IGF1R). LncRNA-MEG3 was ultimately demonstrated to be a new biomarker and therapeutic target of HPH [24]. In addition, miR-483 [18], miR-182-3p [19], miR-125-5p [20], circRNA CDR1as [22], hsa_circ_0016070 [25] and circ-calm4 [18] were identified to function through RNA-RNA interactions in mediating the pathogenesis of HPH or pulmonary artery hypertension (PAH). Nevertheless, the overall RNA interacting network at transcriptomic level in pulmonary arteries of HPH rats remains elusive.

Moreover, several RNAs, including lncRNA, circRNA and other RNAs were recently proved to interact with each other and act as natural miRNA sponges to form competing endogenous RNA (ceRNA) network that participating in the regulation of many biological processes [26, 27]. However, the role of ceRNA network in regulating the remodelling of pulmonary artery during HPH development has not been characterized.

To reveal the ceRNA regulation network in HPH progression, we profiled transcriptome (mRNAs, lncRNAs, circRNAs and miRNAs) in the pulmonary arteries of HPH rats as well as the normal controls. According to the workflow in this study (Fig. 1), differentially expressed miRNAs (DEmiRNAs) were identified as potential hub genes for constructing ceRNA regulatory network through predicting their interacting relationships with other differentially expressed RNAs (DERNAs). Furthermore, functional enrichment and protein-protein interaction (PPI) analysis were also conducted to identify the hub proteins and elucidate possible regulatory mechanism in HPH development. DERNAs involved in ceRNA regulatory network was then validated through real-time reverse transcription-PCR (qRT-PCR). Potential hub mRNAs were finally evaluated for their expression profiles and diagnostic effectiveness in patients with PAH. Our study, for the first time, revealed the ceRNA regulatory network occurred in pulmonary artery during HPH development, and identified potential dysregulated mRNAs for PAH diagnosis. We hope the results from this study may pave the way for the discovery of novel diagnostic biomarkers and therapeutic targets of HPH.

Results

Construction of HPH rat model

In order to construct the HPH rat model, healthy rats were exposed to chronic hypoxia, and body weight, right ventricular pressure (RVSP) and right ventricular hypertrophy index (RVHI) of the rats were evaluated at 21 days after hypoxia. Two batches of HPH rats were constructed in this study, the first batch of HPH rats were used for high throughput RNA (mRNAs, lncRNAs, circRNAs and miRNAs) sequencing, whereas the second batch of HPH rats were utilized for qRT-PCR validation. RVSP and RVHI were significantly increased in first batch of HPH rats compared with that in the control group (**Fig. 2A, B**). Moreover, obvious pulmonary vascular remodelling in HPH rats was confirmed by hematoxylin and eosin (H&E) staining and increased wall thickness of pulmonary artery (**Fig. 2C**). Similar induction of the HPH rats was also observed for the second batch of rats (**Additional file 1: Table S1**).

Identification of differentially expressed RNAs (DERNAs)

Pulmonary arteries from both HPH and normal rats were separated from connective tissues and cleaned for total RNA isolation, which was then subjected to whole transcriptome sequencing and miRNA sequencing respectively.

Clean reads were generated through quality control of the raw sequencing reads, and were then mapped to the primary assembly of rat genome (RGSC 6.0), and mature rat miRNA sequences listed in miRbase (*www.mirbase.org*, release 22) (**Additional file 1: Table S2**). To assess the reliability of sequencing result, principal component analysis (PCA) was conducted to analyse the expression profiles of all identified RNAs (mRNAs, lncRNAs, circRNAs and miRNAs), clear separation between hypoxic and normal samples was observed (**Fig. 3A-D**), suggesting the applicability of the data for further analysis.

To eliminate those inconsistencies and variations among samples, a strict criterion was set to identify DERNAs between HPH and control rats in this study. In general, we first filtered the relatively low expressed RNAs by dropping those RNAs with median fragments per kilo base per million mapped reads (FPKM) or transcript per million (TPM) value less than 10 for mRNAs (FPKM), 5 for lncRNAs (FPKM), circRNAs (TPM) and miRNAs (TPM) among all tested samples. Then screening for DERNAs (> 2-fold change and $padj < 0.05$ for mRNAs; > 1-fold change and $p < 0.05$ for lncRNAs, circRNAs and miRNAs) were performed, 19 significant DEmRNAs (13 up- and 6 downregulated), 8 significant DElncRNAs (5 up- and 3 downregulated), 19 significant DEcircRNAs (9 up- and 10 downregulated) and 23 DEmiRNAs (17 up- and 6 downregulated) were eventually identified in pulmonary arteries of the HPH rats compared with the control rats. Volcano plot suggested the significant differences relative to the magnitude of every single gene between HPH and control groups. In addition (**Fig. 3E-H**), heatmap of the significant dysregulated RNAs showed hierarchical clustering between HPH and normal control rats (**Fig. 3I-L**).

Gene ontology and KEGG pathway analyses

To further characterize the regulatory network in pulmonary artery upon hypoxia, gene ontology (GO) and Kyoto Encyclopedia of genes and genomes (KEGG) pathway analyses were conducted for the DEmRNAs (> 1-fold change and *padj* < 0.05). Top 10 enriched GO terms were mainly associated with positive regulation of cell adhesion (gene ratio = 22/162, *p* =1.54E-10), cell-substrate adhesion (gene ratio = 21/162, *p* = 2.04E-11), external encapsulating structure (gene ratio = 15/160, *p* = 2.87E-06), myofibril (gene ratio = 13/160, *p* = 1.40E-07), actin binding (gene ratio = 14/154, *p* = 3.67E-05), cell adhesion molecule binding (gene ratio = 12/154, *p* = 1.26E-05) and so on (**Fig. 4A; Additional file 1: Table S3**).

Moreover, top 10 KEGG pathways (*p* < 0.05) with the highest gene ratio were also identified (**Fig. 4B**), including cell adhesion molecules (gene ratio = 8/90, *p* = 0.00034), axon guidance (gene ratio = 7/90, *p* = 0.00236), salivary secretion (gene ratio = 7/90, *p* = 0.00016), PPAR signalling pathway (gene ratio = 6/90, *p* = 0.00022), fluid shear stress and atherosclerosis (gene ratio = 6/90, *p* = 0.00424), kaposi sarcoma-associated herpesvirus infection (gene ratio = 6/90, *p* = 0.02227), calcium signalling pathway (gene ratio = 6/90, *p* = 0.033673612), mineral absorption (gene ratio = 5/90, *p* = 0.00024), viral myocarditis (gene ratio = 5/90, *p* = 0.00167), retinol metabolism (gene ratio = 5/90, *p* = 0.00176) and so on (**Additional file 1: Table S4**). As the enriched pathways were usually present in cancer cells during their proliferation or metastasis, these results further suggested the cancer-like pathobiology in pulmonary arteries of HPH rats.

Construction of a potential lncRNA/circRNA-miRNA-mRNA ceRNA regulatory network

According to the ceRNA hypothesis, lncRNAs could compete with circRNAs for same miRNAs and further impact downstream gene expression. To obtain the competing relationship, we predicted the interacting possibilities between DElncRNAs-DEmiRNAs, DEcircRNAs-DEmiRNAs and DEmiRNAs-DEmRNAs. We found that a total of 10 DEmiRNAs (9 up- and 1 downregulated) could be targeted by 7 DElncRNAs (4 up- and 3 downregulated) and 6 DEcircRNAs (6 downregulated). Furthermore, these DEmiRNAs could target to 18 DEmRNAs (13 up- and 5 downregulated) (**Table 1**). At last, an lncRNA/circRNA-miRNA-mRNA ceRNA regulatory network that respond in the pulmonary arteries of HPH rats was constructed based on the interacting relationships (**Fig. 5A**), which was composed of 41 nodes and 86 connections.

In addition, the co-expression pattern of the DEmRNAs that involved in the ceRNA network were also investigated. We found seven co-expression gene pairs including HopX-Clic5、HopX-Ager、Clic5-Cyy1、Clic5-Ager、Cldn18-Ager、Postn-Ltbp2、Postn-Ccl21 (**Fig. 5B**). Furthermore, PPI analysis of the DEmRNAs suggested the hub role of Postn, Spp1, Ager, Aqp5, Clic5 and HopX in mediating the response of pulmonary artery to hypoxia (**Fig. 5C**).

Validation of DERNAs in ceRNA network

To validate the potential interactions and expression profiles of DERNAs in the ceRNA network, the expression level of selected miRNAs that involved in ceRNAs were verified by qRT-PCR on another eleven independent pulmonary arteries separated from HPH and normal control rats. The expression of rno-miR-1247-5p, rno-miR-127-3p, rno-miR-199a-5p, rno-miR-205, Postn, Ltbp2 and Spp1 were demonstrated to be

upregulated, which was as expected according to the sequencing results (**Fig. 6A-D, I, J, L**). Moreover, expression profiles of circ_0001188, circ_0004345 and circ_0002500 and LINC1589 were also proved to be in consistent with the sequencing result (**Fig. 6E-H, K**). These results further supported the miRNA-hub ceRNA regulatory network constructed in this study.

Identification of the diagnostic hub mRNA for PAH

To further explore whether the pulmonary artery-associated mRNAs in the ceRNA network were associated with clinical diagnosis, the expression of selected hub mRNAs were investigated in the dataset of GSE117261, which recorded gene expression profiles in the lung tissues of 25 normal individuals, 32 patients with idiopathic PAH (IPAH); 5 patients with heritable PAH (HPAH), 17 connective tissue disease, congenital heart defects, anorexigen/stimulant drug use-associated PAH (APAH). Finally, 4 DEmRNAs were found significantly dysregulated in PAH. Higher expression of latent transforming growth factor beta binding protein 2 (LTBP2) and periostin (POSTN) were found in all PAH patients (**Fig. 7A, B**), whereas lower expression of secreted phosphoprotein 1 (SPP1) and limbic system associated membrane protein (LSAMP) were found in most of the PAH patients except the HPAH patients (**Fig. 7C, D**). Moreover, the diagnostic value of LTBP2, POSTN, SPP1 and LSAMP in differentiating PAH tissues from normal tissues was evaluated. LTBP2 and POSTN were found to be upregulated in both pulmonary arteries of HPH rats and lung tissues of PAH patients. Area under the curve (AUC) of 0.8333 (95% confidence interval (CI): 0.7429-0.9237) for LTBP2 and AUC of 0.8319 (95% CI: 0.7336-0.9301) for POSTN were identified (**Fig. 7E, F**). Although SPP1 was found to have opposite expression pattern in pulmonary arteries of HPH rats and lung tissues of PAH patients compared with corresponding normal controls, it exhibited the best diagnostic effectiveness with AUC of 0.8652(95% CI: 0.7723-0.9580) (**Fig. 7G**). Similarly, LSAMP was found to have the AUC of 0.747 (95% CI: 0.6300-0.8648) in diagnosing PAH (**Fig. 7H**).

Discussion

With the increasing incidence and prevalence of HPH reported in the last decade [3, 4], a more intensive understanding of the molecular mechanism during HPH development is required for achieving better diagnosis and therapy. In this study, we constructed a transcriptomic regulatory network based on high throughput RNA sequencing results of pulmonary arteries from HPH rats. We hope that the ceRNA network identified in this study could provide comprehensive and novel insights into the pathogenesis as well as potential therapeutic targets of HPH.

In this study, only high expressed RNAs were used for differentially expression analysis so as to eliminate variations presented in HPH rats. DEmRNAs (> 1-fold change and *padj* < 0.05) identified in pulmonary arteries were proved to participate in cell adhesion, axon guidance, PPAR signalling pathway and calcium signalling pathway after hypoxia. In accordance with our findings, DEmRNAs such as Vegfa[28], Ager [29], Ltbp2 [30], Postn [31], Atp2b4 [32] and Ccl21 [33] have been previously reported dysregulated during HPH or PAH development. Although lncRNAs and circRNAs were found to have much lower expression compared with mRNAs, 8 novel DElncRNAs and 19 novel DEcircRNAs that responded to hypoxia in

pulmonary arteries were also observed. In addition, alterations of 23 miRNAs were found after hypoxia, among which miR-20a-5p [34], miR-199a-5p [35], miR-34c-5p [36] and miR-214-3p [37] were reported to be involved in the process of vascular remodelling. Profiling of these DERNAs in pulmonary artery indicated that significant alterations of RNA expression occurred upon hypoxia, which might contribute to the pathophysiology of HPH.

Growing evidence suggested that lncRNAs and circRNAs with miRNA binding sties (MREs) could compete with mRNAs for binding to miRNAs, thereby regulating the RNA expression and affecting disease progression. Despite ceRNA network and lncRNA-miRNA interactions have been reported in the lung tissue of HPH [38–40], the crosstalk of lncRNA/circRNA-miRNA-mRNA in pulmonary arteries of HAH rats has never been investigated.

Upon obtaining the DERNAs in pulmonary arteries of HPH rats, DEmiRNAs were selected as hub nodes for predicting the interacting relationships between DEmiRNAs-DElncRNAs, DEmiRNAs-DEcircRNAs and DEmiRNAs-DEmRNAs. To eliminate the false positive, strict threshold was set to screen for the RNA-RNA interactions. Ten miRNAs were finally identified as hub nodes to compete with 7 lncRNAs and 6 circRNAs for directing the expression of 18 mRNAs.

miR-214-3p has been demonstrated to significantly upregulated and mediated the proliferation and migration of PASMCs upon hypoxia by directly targeting ARHGEF12 [37]. In this study, we further extended the potential regulating axis through introducing 2 lncRNAs that might specifically sponge miR-214-3p to regulate the expression of 6 downstream mRNAs. Moreover, miR-199a-3p has been found to directly target Clic5 and promote cell cycle for cardiomyocyte proliferation and regeneration [41, 42]. The similar regulation axis might also present in pulmonary artery as several miRNAs including miR-199a-3p were supposed to control the expression of Clic5. Interestingly, another lncRNA Hip1-OT1 was predicted to simultaneously sponge miR-541-5p and miR-199a-3p to affect the expression of Clic5. In addition, downregulated miR-34c-5p was also found to regulate the Clic5 expression, and the regulatory axis might consist another novel circular RNA circ_0002500. With emerging evidence showing the critical role of circRNAs in diverse physiological processes, the biological function and molecular diagnostic value of circRNAs in HPH are attracting scientific attention. CircRNA CDR1as was recently demonstrated to upregulate calcium/calmodulin-dependent kinase II-delta (CAMK2D) and calponin 3 (CNN3) through sponging miR-7-5p in PASMCs to promote its calcification [22]. Moreover, hsa_circ_0016070/miR-942/CCND1 regulatory axis was also identified to be associated with HPH through promoting PASMCs proliferation [25]. According to the research result above, we speculated that the DEcircRNAs identified in this study might function synergistically with other DERNAs in the pathogenesis of HPH. According to our hypothesis, both circ_0000873 and circ_0008870 could interact with miR-3543 and thus upregulate the downstream mRNAs including Cldn18, Ager, Napsa and Ltbp2, which were considered to participate in inflammatory and regulation of cell proliferation. Furthermore, circ_0003414/circ_0004345-miR-205, circ_0004345-miR-541-5p, circ_0001188-miR-127-3p, circ_0001188-miR-199a-5p and circ_0002500-miR-34c-5p were predicted to be circRNA-miRNA regulatory pairs as well, which together with the downstream

mRNAs might cooperatively or independently participate as regulatory axis in HPH development. Nevertheless, the biological function and the regulatory mechanisms required further clarification.

GO and KEGG analyses performed in this study focused on the DEmRNAs in pulmonary arteries of HPH rats. The enriched functions and processes include cell adhesion, cell-substrate adhesion, tissue migration, actin binding, glycosaminoglycan binding, extracellular matrix binding and so on. In parallel with GO, KEGG analysis identified cell adhesion molecules, axon guidance, PPAR signalling pathway, calcium signalling pathway and so on. These finding were in consistent with the fact that the pulmonary vascular remodelling was mainly due to proliferation and migration of PASMCs.

PPI analysis via STRING database suggested the key role of Ager, Spp1, Clic5, Aqp5, Postn, Ltbp2 and Hopx in the pulmonary artery in response to hypoxia, which might also be potential diagnostic biomarker and therapeutic targets for HPH. Co-expression of Hopx-Clic5-Ager, Postn-Ltbp2, and Postn-Ccl21 were further identified, suggesting their synergistic function in pulmonary artery during hypoxia. Postn, an extracellular matrix encoding protein that involved in tissue remodelling in response to injury, was found to be upregulated in pulmonary arteries of HPH patients [31]. Accumulated POSTN in nucleus of the endothelial cells upon hypoxia lead to its dysfunction, whereas extracellular POSTN secreted from the cytoplasm promote the proliferation and migration of PASMCs and thus lead to the progression of HPH [31]. Moreover, Postn expression was also reported to increase in RV of monocrotaline (MCT)-induced PAH rats, and increased POSTN could further enhance inducible nitric oxide synthase (iNOS) expression and subsequent nitric oxide (NO) production in right ventricular fibroblast (RVFbs) [43]. Since extracellular matrix remodelling is the key phenomenon in cancer cell invasion and metastasis, the remodelling of pulmonary artery initiated by dysregulated Postn further confirmed the cancer-like pathobiology of PAH. In this study, Postn was predicted to be targeted by miR-205, miR-20a-5p and miR-541, which were speculated to compete with several lncRNAs and circRNAs for binding to Postn. Therefore, lncRNA/circRNA-miRNA-Postn regulatory axis might have actually existed in the development of HPH, and required validation and exploration in the future.

Similarly, expression of Ager was not only found to increase in both human and mouse PASMCs under hypoxia, but also highly upregulated in pulmonary arteries of hypoxia plus SU5416 (HySU)-induced PAH mice [29]. Activation of Ager could facilitate the extracellular matrix (ECM) deposition and disease progression in HPH [29]. The ceRNA network related to Ager identified in this study was composed of 4 miRNAs, 5 lncRNAs and 5 circRNAs. Furthermore, Ltbp2 was found to have diagnostic value for PAH with AUC of 0.8333 (95% CI: 0.7429-0.9237) in this study. Ltbp2 has been demonstrated to be secreted from lung myofibroblasts, and could serve as a biomarker for idiopathic pulmonary fibrosis (IPF) [30]. The circEPSTI1/mir-942-5p/LTBP2 regulatory axis was also identified to affect the proliferation and invasion of oral squamous cell carcinoma (OSCC) cell through the acceleration of epithelial-mesenchymal transition (EMT) and phosphorylation of PI3K/Akt/mTOR signalling pathway[44]. Results from these studies further expanded the possibility of Ltbp2 as a diagnostic marker and therapeutic target in PAH. Considering the fact that one node in the ceRNA network might be involved in multiple regulatory axis, the complex regulatory relationship should be carefully considered and validated.

Nevertheless, limitations of this study should also be taken into consideration. First, the sample size used for profiling DERNAs was relatively small, and thus might lead to increased variations. Second, the RNA-RNA interaction relationships in ceRNA network were based on prediction algorithm that required further experimental validation.

In conclusion, a ceRNA regulatory network in pulmonary artery of HPH rats was constructed, 10 hub miRNAs and their corresponding interacting lncRNAs, circRNAs and mRNAs were identified. The expression profiles of several RNAs involved in the ceRNA network were validated by qRT-PCR. The diagnostic effectiveness of several hub mRNAs was evaluated.

Materials And Methods

Construction of HPH rats and sample collection

Healthy male Sprague-Dawley (SD) rats (8-week-old) were randomly divided into normoxia and hypoxia groups with 5 rats in each group. Rats were exposed to normoxic (21% O2) or hypoxic (10% O2) conditions for 3 weeks respectively. Oxygen concentration were monitored by detecting probe inside the chambers.

To measure RVSP, rats were initially anesthetized, and the right jugular vein was surgically exposed, then a polyethylene catheter connected to AP-621G (Nihon Kohden, Japan) was finally inserted in the right ventricle (RV) for recoding the RVSP by utilizing MP150 system and AcqKnowledge® 4.2.0 software package (BIOPAC Systems, USA).

After hemodynamic measurement, animals were sacrificed and the chest was opened. The lung, heart and pulmonary artery were harvested and washed in clean saline solution at least three times to remove the blood as clean as possible. The pulmonary artery was separated from one lobe of lung and immediately frozen in liquid nitrogen for RNA isolation. Another lobe of lung was fixed in formalin to prepare paraffin-embedded tissues for H&E staining. To measure RVHI, the RV was separated from the left ventricle (LV) and the ventricular septum (S). The RVHI was calculated as ratio of RV weight to the LV plus S weight.

Whole transcriptome sequencing

Total RNA from pulmonary arteries were isolated with RNAiso Plus (Takara, Japan) and dissolved in RNase-free water according to the instructions provided by the manufacturer. Quality control were conducted for the total RNA through measuring the concentration of RNA by the NanoDrop 2000c Spectrophotometer (Thermo Fisher Scientific, USA), detecting the DNA contamination by gel electrophoresis system EPS 601 (GE Healthcare, USA), evaluating the RNA integrity by Agilent 2100 bioanalyzer (Agilent, USA).

Library construction and sequencing for characterizing mRNA, lncRNA and circRNA expression was carried out by Novogene Biotechnology Corporation (Beijing, China). In general, sequencing libraries was

constructed with 5 μg qualified total RNA as input material. Ribosomal RNA was removed from total RNA, and then the rRNA-depleted RNA was fragmented to 200-300 base pairs (bps). First strand cDNA was synthesized using random hexamer primers and Moloney Murine Leukemia (M-MuLV) reverse transcriptase (RNaseH-), and second strand cDNA synthesis was subsequently performed using DNA polymerase I and RNase H in the reaction buffer with dUTP instead of dTTP. End repair, dA-tailing, adaptor ligation and size-selection were performed for the double strand cDNA, then library amplification was conducted following USER enzyme treatment, which was subjected to purification. Quality of the library was finally assessed by the Agilent Bioanalyzer 2100 system (Agilent, USA).

Library construction and sequencing for characterizing miRNA expression was carried out following the S-Poly (T) method described in our previous study with some modifications[45]. In general, sequencing library was constructed from starting material of 500 ng qualified total RNA. One-step poly-adenylation and reverse transcription (Poly(A)/RT) were performed with 5 μl of 4× reaction buffer, 1 μl 2.5 μlM RT primer, and 1 μl Poly(A)/RT enzyme, the reaction was incubated at 37 °C for 30 min, which was similar to the methods described before [45]. Then the exonuclease I (New England Biolabs, USA) was used to eliminate the remaining RT primers. Frist stand cDNA was then ligated to a splint adapter with a random single-stranded overhang and ligation blocking modification according to the method reported previously [46]. Amplification was then executed for the cDNA to generate miRNA sequencing library, which was subjected to purification by AMpure XP beads (Beckman, USA) to select DNA fragments with averaged size of approximately 180 to 200 bps. Quality of the library was finally assessed by the Agilent Bioanalyzer 2100 system (Agilent, USA).

Raw sequencing data treatment

Clean reads were obtained through removing raw reads containing adapter and poly-N sequences using in-house python scripts. In addition, low quality reads were also eliminated as well. Mapping of the clean reads to rat genome, transcriptome and mature miRNA sequences from miRbase was performed by using Hisat2 (v2.0.5) or bowtie2 (v2.0.6) [47]. For characterizing transcripts of mRNA, lncRNA and circRNA, the mapped reads from each sample were assembled by StringTie (v1.3.3) in a reference-based manner. The following principles were used to identify novel lncRNAs: (1) more than 2 exons were found in the transcript; (2) the length of the transcript was larger than 200 bp; (3) coding potential of the transcript was found by CNCI (Coding-Non-Coding-Index) (v2), CPC (Coding Potential Calculator) (cpc-0.9-r2) and PFAM (Pfam Scan) (v1.3) simultaneously. Furthermore, overlapping circRNAs identified by both find_circ and CIRI (V2.0.5) from each sample were considered as novel circRNAs. Reads mapped to mRNA, lncRNA and circRNA were counted by StringTie (v1.3.3). For characterizing miRNA expression, reads mapped to mature miRNA sequence were counted by in-house python script. The expression of mRNA, lncRNA, circRNA and miRNA were calculated using FPKM and TPM methods respectively.

Identification of DERNAs

Median FPKM or TPM value among all tested samples was calculated for each mRNA, lncRNA, circRNA and miRNA. Threshold of 10 for mRNAs, 5 for lncRNAs, circRNAs and miRNAs were used to eliminate low

expressed RNAs. After selecting the pre-treated data, DEmRNAs (> 2-fold change and *padj* < 0.05), DElncRNAs (> 1-fold change and *p* < 0.05), DEcircRNAs (> 1-fold change and *p* < 0.05) and DEmiRNAs (> 1-fold change and *p* < 0.05) were determined by DEseq2 (v1.32.0) R package. DERNAs were then illustrated in volcano and heatmap by ggplot2 (v3.3.3) and pheatmap (v1.0.12) R packages.

Gene function annotation

GO analysis was conducted based on DEmRNAs (> 1-fold change and *padj* < 0.05) to evaluate enrichment for biological processes (BP), cellular component (CC), and molecular function (MF) annotations with clusterProfiler (v4.0.0) R package. KEGG analysis was also performed to enrich the signalling pathways associated with DEmRNAs (> 1-fold change and *padj* < 0.05) using clusterProfiler (v4.0.0) R package. GO terms and KEGG pathways with enriched genes ≥2 and *p* < 0.05 were selected for further analysis. Top 10 ranked GO terms and KEGG pathways containing most genes were visualized by ggplot2 (v3.3.3) R package.

Prediction of targeting relationship

RNA regulatory network among 19 DEmRNAs, 8 DElncRNAs, 19 DEcircRNAs and 23 DEmiRNAs were predicted by multiple approaches. In general, the DEmiRNAs were selected as the hub components for constructing ceRNA regulatory network (Table 1). Targeting relationships between DEmiRNAs-DEmRNAs, DEmiRNAs-DElncRNAs, DEmiRNAs-DEcircRNAs were predicted mainly based on miRanda (v1.0b, -sc 100; -en -20). In addition, miRcode (*http://mircode.org/*), TargetScan (*http://www.targetscan.org/*), starBase (*http://starbase.sysu.edu.cn/*) and CircInteractome (*https://circinteractome.irp.nia.nih.gov/*) were also exploited to confirm the targeting relationships. The overlapping DEmiRNAs predicted in all the three RNA-RNA pairs were then used as core node to build the initial ceRNA regulatory network in Cytoscape (v3.8.2).The complete circRNA/lncRNA-miRNA-mRNA regulatory network was finally constructed based on the predicted targeting relationships between miRNAs and other RNAs.

Quantitative real-time PCR

To evaluate mRNA, lncRNA and circRNA expression profiles, first strand cDNA was reverse transcribed with oligo (dT) plus random hexamer primers using M-MuLV reverse transcriptase (FAPON, China). Quantitative real-time PCR was conducted on ABI StepOne plus real-time PCR system (Applied Biosystems, USA) with SYBR green master PCR mix and gene-specific primers. Expression levels of targeted genes were normalized by reference gene (β-actin). For miRNA expression profile evaluation, methods described in our previous study was utilized with snoRNA-202 as reference [45, 48]. Relative expression of all RNAs were calculated according to the $2^{-\triangle\triangle Ct}$ method. All primers used in this study were listed in Additional file 1: Table S5.

Diagnostic evaluation of hub DEmRNAs

The mRNA expression dataset of PAH patients (GSE117261) was downloaded from the Gene Expression Omnibus (GEO) database, which includes gene expression profiles of lung tissues from 58 PAH patients (32 patients with idiopathic PAH (IPAH); 5 patients with heritable PAH (HPAH), 17 patients with connective tissue disease, congenital heart defects, anorexigen/stimulant drug use-associated PAH (APAH) and 4 uncharacterized patients) and 25 normal individuals The normalized gene expression pattern of selected genes was analysed using GraphPad Prism 8.0.1. The diagnostic value of hub DEmRNAs was analysed through establishing a receiver operating characteristic (ROC) according to their gene expression profile using GraphPad Prism 8.0.1. The AUC value of ROC curve was calculated for determining the diagnostic effectiveness.

Abbreviations

ceRNA: competitive endogenous RNA; HPH: hypoxia-induced pulmonary hypertension; DERNAs: differentially expressed RNAs; PAH: pulmonary artery hypertension; GEO: Gene Expression Omnibus; PASMCs: pulmonary artery smooth muscle cells; IGF1R, insulin-like growth factor receptor; PPI, protein-protein interaction; qRT-PCR: real-time reverse transcription-PCR; RVSP: right ventricular pressure; RVHI: right ventricular hypertrophy index; H&E: hematoxylin and eosin; FPKM: fragments per kilo base per million mapped reads; TPM: transcript per million; GO: gene ontology; KEGG: Kyoto Encyclopedia of genes and genomes; HPAH: heritable PAH; APAH: associated PAH; LTBP2: latent transforming growth factor beta binding protein 2; POSTN: periostin; SPP1: secreted phosphoprotein 1; LSAMP: limbic system associated membrane protein; AUC: area under the curve; CI: confidence interval; MREs: miRNA binding sties; CAMK2D: calcium/calmodulin-dependent kinase II-delta; CNN3: calponin 3; MCT: monocrotaline; iNOS: inducible nitric oxide synthase; NO: nitric oxide; RVFbs: right ventricular fibroblasts; HySU: hypoxia plus SU5416; ECM: extracellular matrix; IPF: idiopathic pulmonary fibrosis; OSCC: oral squamous cell carcinoma; EMT: epithelial-mesenchymal transition; SD: Sprague-Dawley; CNCI: coding-non-coding-index; CPC: coding potential calculator; PFAM: Pfam Scan; BP: biological processes; CC: cellular component; MF: molecular function; ROC: receiver operating characteristic.

Declarations

Acknowledgements

Not applicable.

Authors' contributions

D.G., L.L. designed the research. L.L., Y.N. Q.C. constructed the HPH rat model. J.W., S.Z., Y.N., L.L. prepared RNA for whole transcriptome RNA sequencing and miRNA sequencing libraries. J.W., Y.N. Q.G. performed the qRT-PCR validation. J.W., Z.L. conducted comprehensive bioinformatics analyses. J.W. and D.G. wrote the manuscript, and all authors participated in discussion, data interpretation, and manuscript editing.

Funding

This work was supported by National Natural Science Foundation of China (91739109, 81970053, 81570046, 81870045 and 81700054); Guangdong Provincial Key Laboratory of Regional Immunity and Diseases (2019B030301009); Shenzhen Municipal Basic Research Program (JCYJ20190808123219295 and JCYJ20170818144127727); Interdisciplinary Innovation Team Project of Shenzhen University (843-00000325), Science and Technology Project of Shenzhen Nanshan District (Health Care, 2018012), and the start-up funds from Shenzhen University (to J.W.).

Ethics approval and consent to participate

Rats used in this study were purchased from Guangdong Medical Laboratory Animal Center (Guangzhou, China). All experiments followed protocols that approved by animal care committee of Shenzhen University, China.

Availability of data and materials

NGS data will be deposited in NCBI's Sequence Read Archive (SRA) and are available through SRA accession number no. upon acceptance.

Consent for publication

All author shave agreed to publish this manuscript.

Competing interests

The authors declare no conflict of interest.

Author details

[1]Shenzhen Key Laboratory of Microbial Genetic Engineering, Vascular Disease Research Center, College of Life Sciences and Oceanography, Guangdong Provincial Key Laboratory of Regional Immunity and Disease, Carson International Cancer Center, School of Medicine, Shenzhen University, Shenzhen, 518060, China.

References

1. Farber HW, Loscalzo J: **Pulmonary arterial hypertension**. *N Engl J Med* 2004, **351**(16):1655-1665.
2. Tuder RM: **Pulmonary vascular remodeling in pulmonary hypertension**. *Cell Tissue Res* 2017, **367**(3):643-649.
3. Lau EMT, Giannoulatou E, Celermajer DS, Humbert M: **Epidemiology and treatment of pulmonary arterial hypertension**. *Nat Rev Cardiol* 2017, **14**(10):603-614.

4. Jiang X, Jing ZC: **Epidemiology of pulmonary arterial hypertension**. *Curr Hypertens Rep* 2013, **15**(6):638-649.
5. Santos-Ferreira CA, Abreu MT, Marques CI, Gonçalves LM, Baptista R, Girão HM: **Micro-RNA Analysis in Pulmonary Arterial Hypertension: Current Knowledge and Challenges**. *JACC Basic Transl Sci* 2020, **5**(11):1149-1162.
6. Sun Z, Liu Y, Yu F, Xu Y, Yanli L, Liu N: **Long non-coding RNA and mRNA profile analysis of metformin to reverse the pulmonary hypertension vascular remodeling induced by monocrotaline**. *Biomed Pharmacother* 2019, **115**:108933.
7. Wang J, Feng W, Li F, Shi W, Zhai C, Li S, Zhu Y, Yan X, Wang Q, Liu L *et al*: **SphK1/S1P mediates TGF-β1-induced proliferation of pulmonary artery smooth muscle cells and its potential mechanisms**. *Pulm Circ* 2019, **9**(1):2045894018816977.
8. Goncharov DA, Kudryashova TV, Ziai H, Ihida-Stansbury K, DeLisser H, Krymskaya VP, Tuder RM, Kawut SM, Goncharova EA: **Mammalian target of rapamycin complex 2 (mTORC2) coordinates pulmonary artery smooth muscle cell metabolism, proliferation, and survival in pulmonary arterial hypertension**. *Circulation* 2014, **129**(8):864-874.
9. Guo ML, Kook YH, Shannon CE, Buch S: **Notch3/VEGF-A axis is involved in TAT-mediated proliferation of pulmonary artery smooth muscle cells: Implications for HIV-associated PAH**. *Cell Death Discov* 2018, **4**:22.
10. Tu L, Desroches-Castan A, Mallet C, Guyon L, Cumont A, Phan C, Robert F, Thuillet R, Bordenave J, Sekine A *et al*: **Selective BMP-9 Inhibition Partially Protects Against Experimental Pulmonary Hypertension**. *Circ Res* 2019, **124**(6):846-855.
11. Weiss A, Neubauer MC, Yerabolu D, Kojonazarov B, Schlueter BC, Neubert L, Jonigk D, Baal N, Ruppert C, Dorfmuller P *et al*: **Targeting cyclin-dependent kinases for the treatment of pulmonary arterial hypertension**. *Nat Commun* 2019, **10**(1):2204.
12. Calvier L, Boucher P, Herz J, Hansmann G: **LRP1 Deficiency in Vascular SMC Leads to Pulmonary Arterial Hypertension That Is Reversed by PPARγ Activation**. *Circ Res* 2019, **124**(12):1778-1785.
13. Legchenko E, Chouvarine P, Borchert P, Fernandez-Gonzalez A, Snay E, Meier M, Maegel L, Mitsialis SA, Rog-Zielinska EA, Kourembanas S *et al*: **PPARγ agonist pioglitazone reverses pulmonary hypertension and prevents right heart failure via fatty acid oxidation**. *Science translational medicine* 2018, **10**(438):eaao0303.
14. Su H, Xu X, Yan C, Shi Y, Hu Y, Dong L, Ying S, Ying K, Zhang R: **LncRNA H19 promotes the proliferation of pulmonary artery smooth muscle cells through AT(1)R via sponging let-7b in monocrotaline-induced pulmonary arterial hypertension**. *Respir Res* 2018, **19**(1):254.
15. Omura J, Habbout K, Shimauchi T, Wu WH, Breuils-Bonnet S, Tremblay E, Martineau S, Nadeau V, Gagnon K, Mazoyer F *et al*: **Identification of Long Noncoding RNA H19 as a New Biomarker and Therapeutic Target in Right Ventricular Failure in Pulmonary Arterial Hypertension**. *Circulation* 2020, **142**(15):1464-1484.

16. Wang D, Xu H, Wu B, Jiang S, Pan H, Wang R, Chen J: **Long non-coding RNA MALAT1 sponges miR-124-3p.1/KLF5 to promote pulmonary vascular remodeling and cell cycle progression of pulmonary artery hypertension**. *Int J Mol Med* 2019, **44**(3):871-884.
17. Wang H, Qin R, Cheng Y: **LncRNA-Ang362 Promotes Pulmonary Arterial Hypertension by Regulating miR-221 and miR-222**. *Shock* 2020, **53**(6):723-729.
18. Liu MC, Oxnard GR, Klein EA, Swanton C, Seiden MV, Liu MC, Oxnard GR, Klein EA, Smith D, Richards D *et al*: **Sensitive and specific multi-cancer detection and localization using methylation signatures in cell-free DNA**. *Ann Oncol* 2020, **31**(6):745-759.
19. Sun L, Lin P, Chen Y, Yu H, Ren S, Wang J, Zhao L, Du G: **miR-182-3p/Myadm contribute to pulmonary artery hypertension vascular remodeling via a KLF4/p21-dependent mechanism**. *Theranostics* 2020, **10**(12):5581-5599.
20. Cai Z, Li J, Zhuang Q, Zhang X, Yuan A, Shen L, Kang K, Qu B, Tang Y, Pu J *et al*: **MiR-125a-5p ameliorates monocrotaline-induced pulmonary arterial hypertension by targeting the TGF-β1 and IL-6/STAT3 signaling pathways**. *Exp Mol Med* 2018, **50**(4):1-11.
21. Li Y, Ren W, Wang X, Yu X, Cui L, Li X, Zhang X, Shi B: **MicroRNA-150 relieves vascular remodeling and fibrosis in hypoxia-induced pulmonary hypertension**. *Biomed Pharmacother* 2019, **109**:1740-1749.
22. Ma C, Gu R, Wang X, He S, Bai J, Zhang L, Zhang J, Li Q, Qu L, Xin W *et al*: **circRNA CDR1as Promotes Pulmonary Artery Smooth Muscle Cell Calcification by Upregulating CAMK2D and CNN3 via Sponging miR-7-5p**. *Mol Ther Nucleic Acids* 2020, **22**:530-541.
23. Zhou S, Jiang H, Li M, Wu P, Sun L, Liu Y, Zhu K, Zhang B, Sun G, Cao C *et al*: **Circular RNA hsa_circ_0016070 Is Associated with Pulmonary Arterial Hypertension by Promoting PASMC Proliferation**. *Mol Ther Nucleic Acids* 2019, **18**:275-284.
24. Xing Y, Zheng X, Fu Y, Qi J, Li M, Ma M, Wang S, Li S, Zhu D: **Long Noncoding RNA-Maternally Expressed Gene 3 Contributes to Hypoxic Pulmonary Hypertension**. *Mol Ther* 2019, **27**(12):2166-2181.
25. Zhou S, Jiang H, Li M, Wu P, Sun L, Liu Y, Zhu K, Zhang B, Sun G, Cao C *et al*: **Circular RNA hsa_circ_0016070 Is Associated with Pulmonary Arterial Hypertension by Promoting PASMC Proliferation**. *Molecular therapy Nucleic acids* 2019, **18**:275-284.
26. Tay Y, Rinn J, Pandolfi PP: **The multilayered complexity of ceRNA crosstalk and competition**. *Nature* 2014, **505**(7483):344-352.
27. Cheng D-L, Xiang Y-Y, Ji L-j, Lu X-J: **Competing endogenous RNA interplay in cancer: mechanism, methodology, and perspectives**. *Tumor Biol* 2015, **36**(2):479-488.
28. Voelkel NF, Gomez-Arroyo J: **The role of vascular endothelial growth factor in pulmonary arterial hypertension. The angiogenesis paradox**. *Am J Respir Cell Mol Biol* 2014, **51**(4):474-484.
29. Jia D, He Y, Zhu Q, Liu H, Zuo C, Chen G, Yu Y, Lu A: **RAGE-mediated extracellular matrix proteins accumulation exacerbates HySu-induced pulmonary hypertension**. *Cardiovasc Res* 2017, **113**(6):586-597.

30. Enomoto Y, Matsushima S, Shibata K, Aoshima Y, Yagi H, Meguro S, Kawasaki H, Kosugi I, Fujisawa T, Enomoto N *et al*: **LTBP2 is secreted from lung myofibroblasts and is a potential biomarker for idiopathic pulmonary fibrosis**. *Clin Sci (Lond)* 2018, **132**(14):1565-1580.
31. Nie X, Shen C, Tan J, Wu Z, Wang W, Chen Y, Dai Y, Yang X, Ye S, Chen J *et al*: **Periostin: A Potential Therapeutic Target For Pulmonary Hypertension?** *Circ Res* 2020, **127**(9):1138-1152.
32. Deng L, Chen J, Wang T, Chen B, Yang L, Liao J, Chen Y, Wang J, Tang H, Yi J *et al*: **PDGF/MEK/ERK axis represses Ca(2+) clearance via decreasing the abundance of plasma membrane Ca(2+) pump PMCA4 in pulmonary arterial smooth muscle cells**. *Am J Physiol Cell Physiol* 2021, **320**(1):c66-c79.
33. Hoffmann-Vold AM, Hesselstrand R, Fretheim H, Ueland T, Andreassen AK, Brunborg C, Palchevskiy V, Midtvedt Ø, Garen T, Aukrust P *et al*: **CCL21 as a Potential Serum Biomarker for Pulmonary Arterial Hypertension in Systemic Sclerosis**. *Arthritis Rheumatol* 2018, **70**(10):1644-1653.
34. Zhou Y, Fang XL, Zhang Y, Feng YN, Wang SS: **miR-20a-5p promotes pulmonary artery smooth muscle cell proliferation and migration by targeting ABCA1**. *J Biochem Mol Toxicol* 2020, **34**(12):e22589.
35. Tian X, Yu C, Shi L, Li D, Chen X, Xia D, Zhou J, Xu W, Ma C, Gu L *et al*: **MicroRNA-199a-5p aggravates primary hypertension by damaging vascular endothelial cells through inhibition of autophagy and promotion of apoptosis**. *Exp Ther Med* 2018, **16**(2):595-602.
36. Xu X, Wang S, Liu J, Dou D, Liu L, Chen Z, Ye L, Liu H, He Q, Raj JU *et al*: **Hypoxia induces downregulation of soluble guanylyl cyclase β1 by miR-34c-5p**. *J Cell Sci* 2012, **125**(24):6117-6126.
37. Xing XQ, Li B, Xu SL, Liu J, Zhang CF, Yang J: **MicroRNA-214-3p Regulates Hypoxia-Mediated Pulmonary Artery Smooth Muscle Cell Proliferation and Migration by Targeting ARHGEF12**. *Med Sci Monit* 2019, **25**:5738-5746.
38. Xu SL, Deng YS, Liu J, Xu SY, Zhao FY, Wei L, Tian YC, Yu CE, Cao B, Huang XX *et al*: **Regulation of circular RNAs act as ceRNA in a hypoxic pulmonary hypertension rat model**. *Genomics* 2021, **113**(1 Pt 1):11-19.
39. Zhu B, Gong Y, Yan G, Wang D, Qiao Y, Wang Q, Liu B, Hou J, Li R, Tang C: **Down-regulation of lncRNA MEG3 promotes hypoxia-induced human pulmonary artery smooth muscle cell proliferation and migration via repressing PTEN by sponging miR-21**. *Biochem Biophys Res Commun* 2018, **495**(3):2125-2132.
40. Zeng Y, Li N, Zheng Z, Chen R, Peng M, Liu W, Zhu J, Zeng M, Cheng J, Hong C: **Screening of Hub Genes Associated with Pulmonary Arterial Hypertension by Integrated Bioinformatic Analysis**. *Biomed Res Int* 2021, **2021**:6626094.
41. Eulalio A, Mano M, Ferro M, Zentilin L, Sinagra G, Zacchigna S, Giacca MJN: **Functional screening identifies miRNAs inducing cardiac regeneration**. *Nature* 2012, **492**(7429):376-381.
42. Ouyang Z, Wei K: **miRNA in cardiac development and regeneration**. *Cell Regen* 2021, **10**(1):14-14.
43. Imoto K, Okada M, Yamawaki H: **Periostin Mediates Right Ventricular Failure through Induction of Inducible Nitric Oxide Synthase Expression in Right Ventricular Fibroblasts from Monocrotaline-Induced Pulmonary Arterial Hypertensive Rats**. *Int J Mol Sci* 2018, **20**(1):62.

44. Wang J, Jiang C, Li N, Wang F, Xu Y, Shen Z, Yang L, Li Z, He C: **The circEPSTI1/mir-942-5p/LTBP2 axis regulates the progression of OSCC in the background of OSF via EMT and the PI3K/Akt/mTOR pathway**. *Cell Death Dis* 2020, **11**(8):682.
45. Niu Y, Zhang L, Qiu H, Wu Y, Wang Z, Zai Y, Liu L, Qu J, Kang K, Gou D: **An improved method for detecting circulating microRNAs with S-Poly(T) Plus real-time PCR**. *Sci Rep* 2015, **5**(1):15100.
46. Aman Da R, Erika M, Per W, Ann-Christine S, Jessica NJNAR: **SPlinted Ligation Adapter Tagging (SPLAT), a novel library preparation method for whole genome bisulphite sequencing**. *Nucleic Acids Res* 2017, **45**(6):e36.
47. Kim D, Langmead B, Salzberg SL: **HISAT: a fast spliced aligner with low memory requirements**. *Nat Methods* 2015, **12**(4):357-360.
48. Brattelid T, Aarnes E-K, Helgeland E, Guvaåg S, Eichele H, Jonassen AK: **Normalization strategy is critical for the outcome of miRNA expression analyses in the rat heart**. *Physiol Genomics* 2011, **43**(10):604-610.

Tables

Table 1. The DERNA interacting relationships in the ceRNA regulatory network.

DEmiRNAs	DEmRNAs	DElncRNAs	DEcircRNAs
rno-miR-1247-5p	Hopx,Sec14l4, LOC108348108,Hspa1b	AABR07000398.1-OT1, LINC5727, Hip1-OT1, RT1-CE7-203	N.A.
rno-miR-127-3p	Ccl21, Ltbp2, Cyyr1, Spp1, Ager, AABR07044412.1	Hip1-OT1, RT1-CE7-203	circ_0001188
rno-miR-199a-3p	Clic5	Hip1-OT1	N.A.
rno-miR-199a-5p	Napsa, Scd, Akap5, Ltbp2, Aqp5, Clic5, Cyyr1, Lsamp, Sec1414, Ager	LINC1589, RT1-CE7-203	circ_0001188
rno-miR-205	Postn, Akap5, Ltbp2, Clic5, Cyyr1, Hopx, Ager	AABR07000398.1-OT1, AC134224.1-201, LINC1589	circ_0003414, circ_0004345
rno-miR-20a-5p	Postn, Clic5, Cyyr1	LINC1589	N.A.
rno-miR-214-3p	Napsa, Akap5, Ltbp2, Clic5, Lsamp, Spp1, Hopx	AC134224.1-201,Ace-202, LINC1589	N.A.
rno-miR-34c-5p	Scd, Ltbp2, Clic5, Cyyr1, Sec14l4	N.A.	circ_0002500
rno-miR-3543	Napsa, Scd, Ltbp2, Cldn18, Cyyr1, Sec14l4, Ager	N.A.	circ_0000873, circ_0008870
rno-miR-541-5p	Napsa, Postn, Akap5, Ltbp2, Clic5, Cyyr1, Lsamp, Hopx, Sec14l4	AABR07000398.1-OT1, LINC1589, Hip1-OT1	circ_0004345

Figures

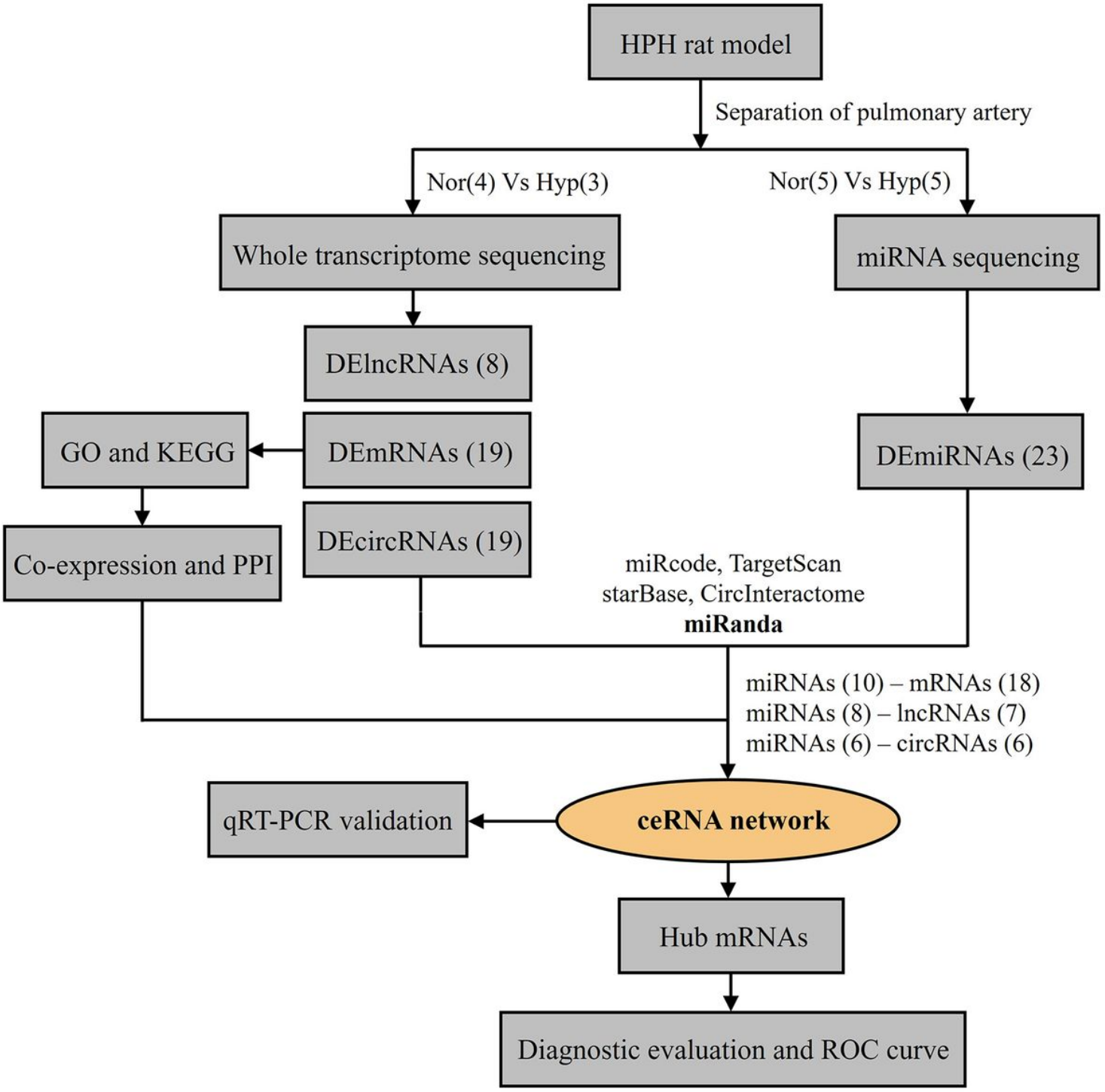

Figure 1

Workflow of the study design. HPH, hypoxia-induced pulmonary hypertension; DElncRNAs, differentially expressed lncRNAs; DEmRNAs, differentially expressed mRNAs; DEcircRNAs, differentially expressed circRNAs; DEmiRNAs, differentially expressed miRNAs; GO, gene ontology; KEGG, Kyoto Encyclopedia of Genes and Genomes; PPI, protein-protein interactions; ceRNA, competing endogenous; qRT-PCR, real-time reverse transcription-PCR; ROC, receiver operating characteristic curve.

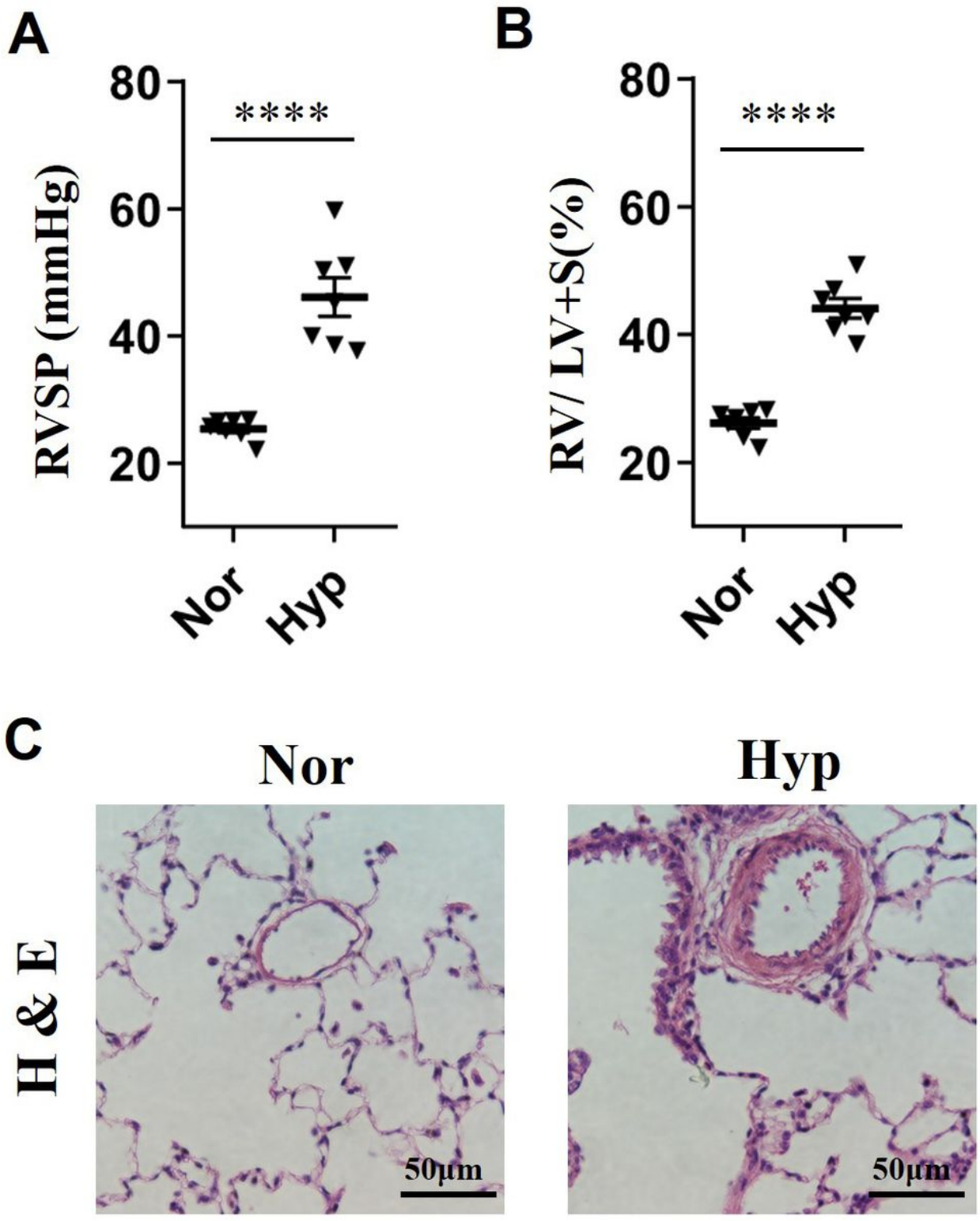

Figure 2

Construction of hypoxia-induced pulmonary hypertension (HPH) rat model. A, The recorded right ventricular pressure (RVSP) of the first batch of HPH rats and normal controls. B, The calculated right ventricular hypertrophy index (RVHI) of the first batch of HPH rats and normal controls. C, Haematoxylin and eosin (H&E) staining of pulmonary arteries from HPH rats and normal controls. Nor, normal control rats; Hyp, HPH rats. ****indicates $p<0.0001$.

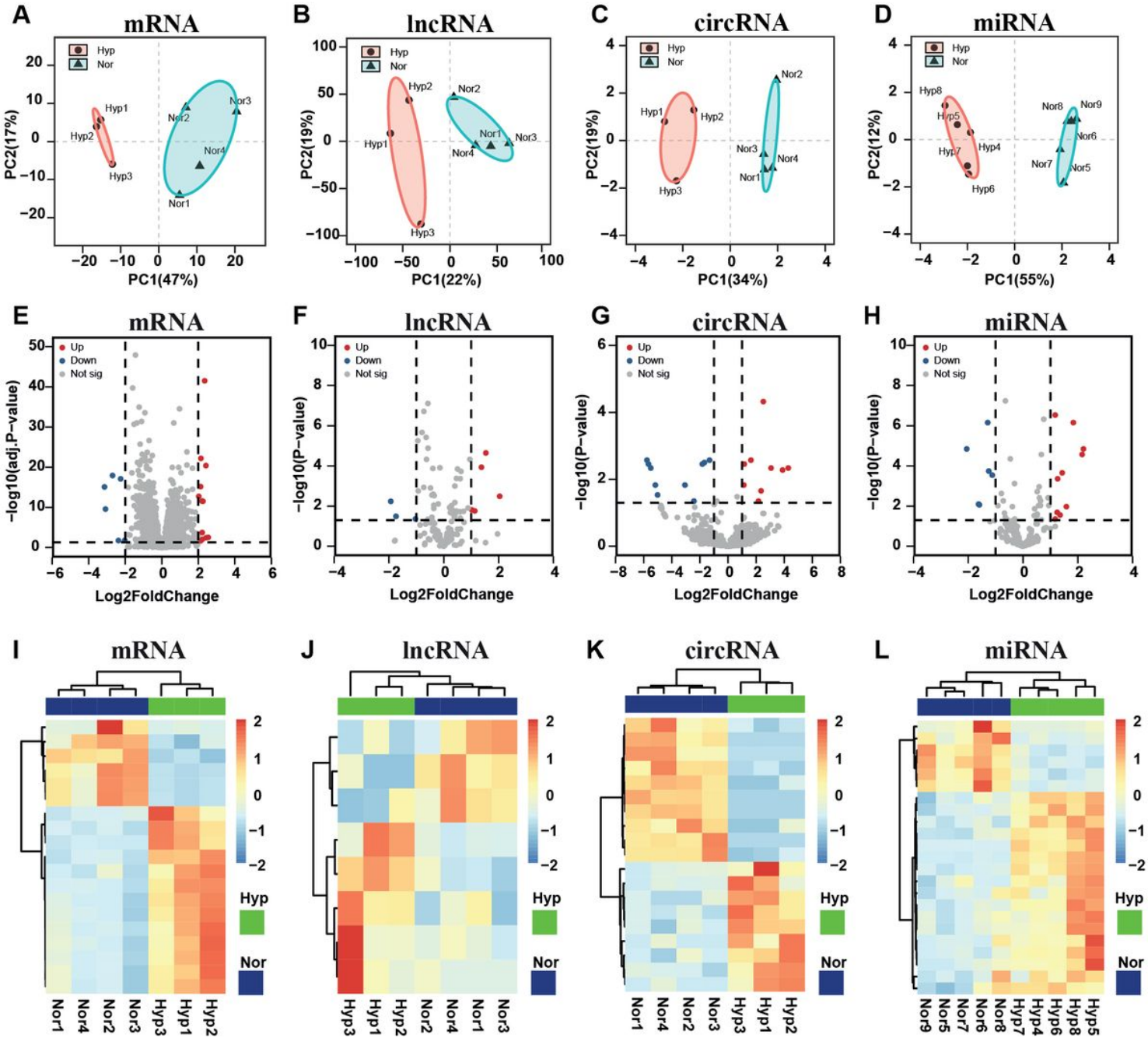

Figure 3

Identification of differentially expressed RNAs (DERNAs). Principal component analysis (PCA) of replicates from both hypoxia-induced pulmonary hypertension (HPH) (red) and control (blue) samples. Samples were clustered according to the expression of 500 most variable mRNAs (A), lncRNAs (B), circRNAs (C) and miRNAs (D) in the sequencing dataset. Ellipses represent 95% confidence intervals for the groups. The volcano plot of DEmRNAs (E), DRlncRNAs (F), DEcircRNAs (G) and DEmiRNAs (H) between HPH and control samples. Red and blue dots represent downregulated and upregulated DERNAs in HPH samples respectively. The horizontal line represents the value of the padj < 0.05 (E) or p < 0.05 (F, G and H); the vertical dotted line represents the value of |Log2FoldChange| > 2 (E) or |Log2FoldChange| >1(F, G and H). Expression heatmap of DEmRNAs (I), DElncRNAs (J), DEcircRNAs (K) and DEmiRNAs (L)

between HPH and control samples. Unsupervised hierarchical clustering analysis of the DERNAs was performed. Orange colour indicates higher expression; blue colour indicates lower expression. Nor, normal control rats; Hyp, HPH rats.

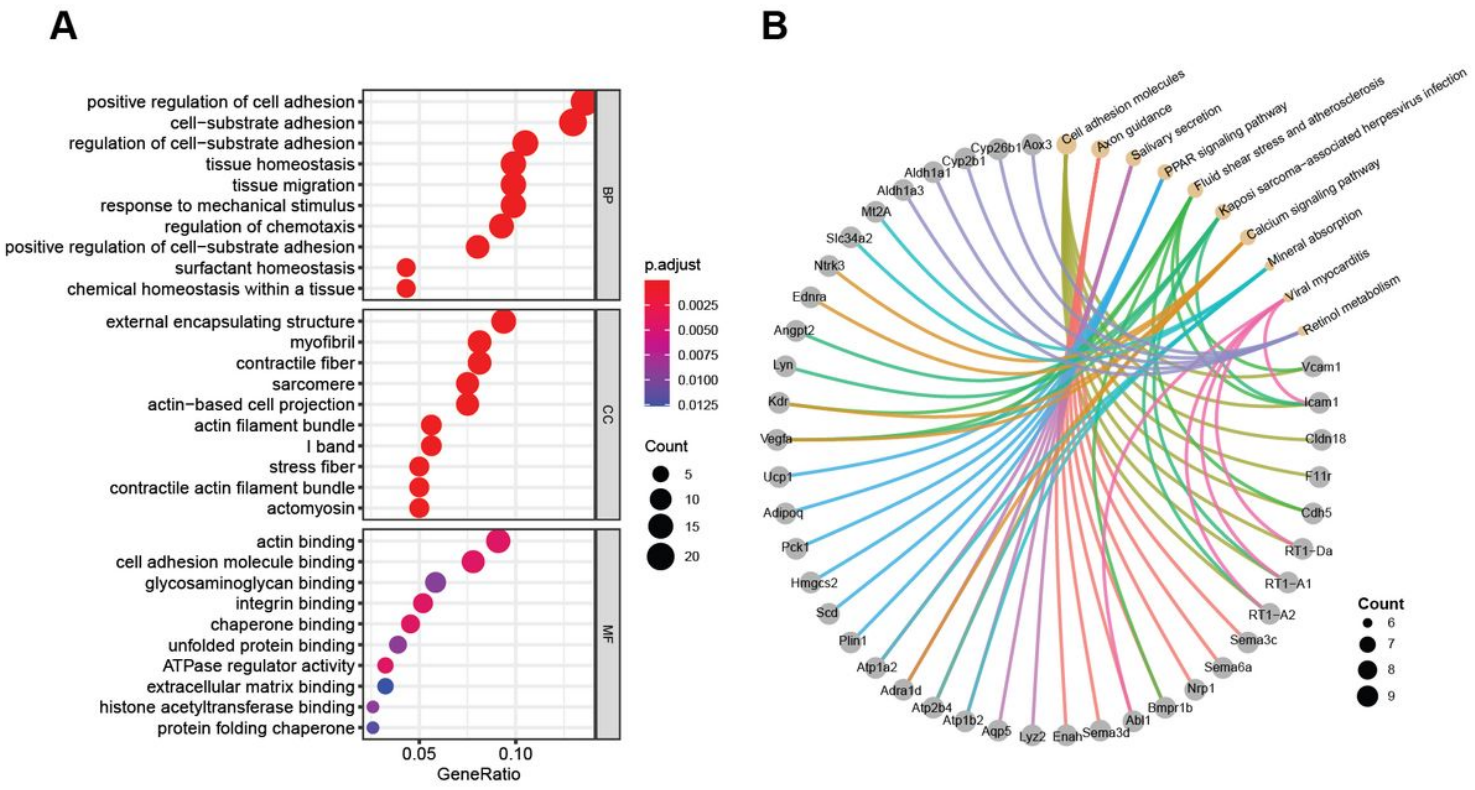

Figure 4

Functional classifications and pathway enrichment analysis of DERNAs. A, Gene ontology (GO) analysis of DEmRNAs between HPH and normal samples. Three aspects including biological process (BP), cellular component (CC), and molecular function (MF) were analysed. B, Kyoto Encyclopedia of genes and genomes (KEGG) pathway analysis of DEmRNAs between HPH and normal samples. Yellow dots indicate the top 10 enriched pathways; grey dots indicate the genes involved in the corresponding pathways.

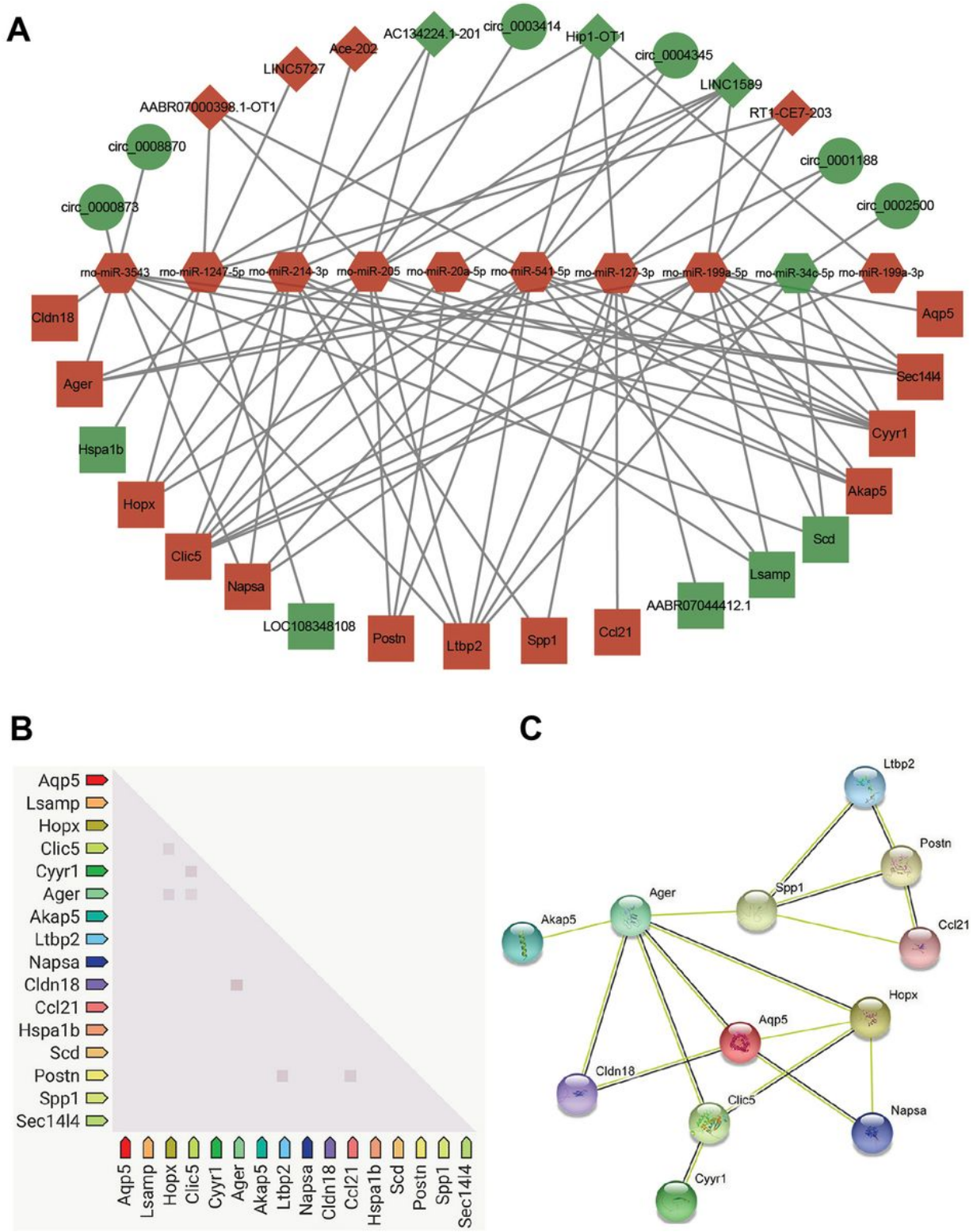

Figure 5

Potential competing endogenous RNA (ceRNA) regulatory network and protein-protein interactions (PPI) analysis in pulmonary artery of HPH rats. A, LncRNA/circRNA-miRNA-mRNA ceRNA regulatory network constructed in this study. The ceRNA regulatory network includs 10 miRNAs, 6 circRNAs, 7 lncRNAs and 18 mRNAs. Red colour indicates upregulated, green colour indicates downregulated; circles indicate cirRNAs, rectangels indicate mRNAs, diamonds indicate lncRNAs, hexagons indicate miRNAs. B, Co-

expression analysis of DEmRNAs by STRING database. The square represent gene association, more intense colour of the square represent a higher association score. C, Results of PPI analysis of DEmRNAs by STRING database. The balls represents the gene nodes, the connecting lines represent the interactions between genes and figures insides the balls represent protein structure.

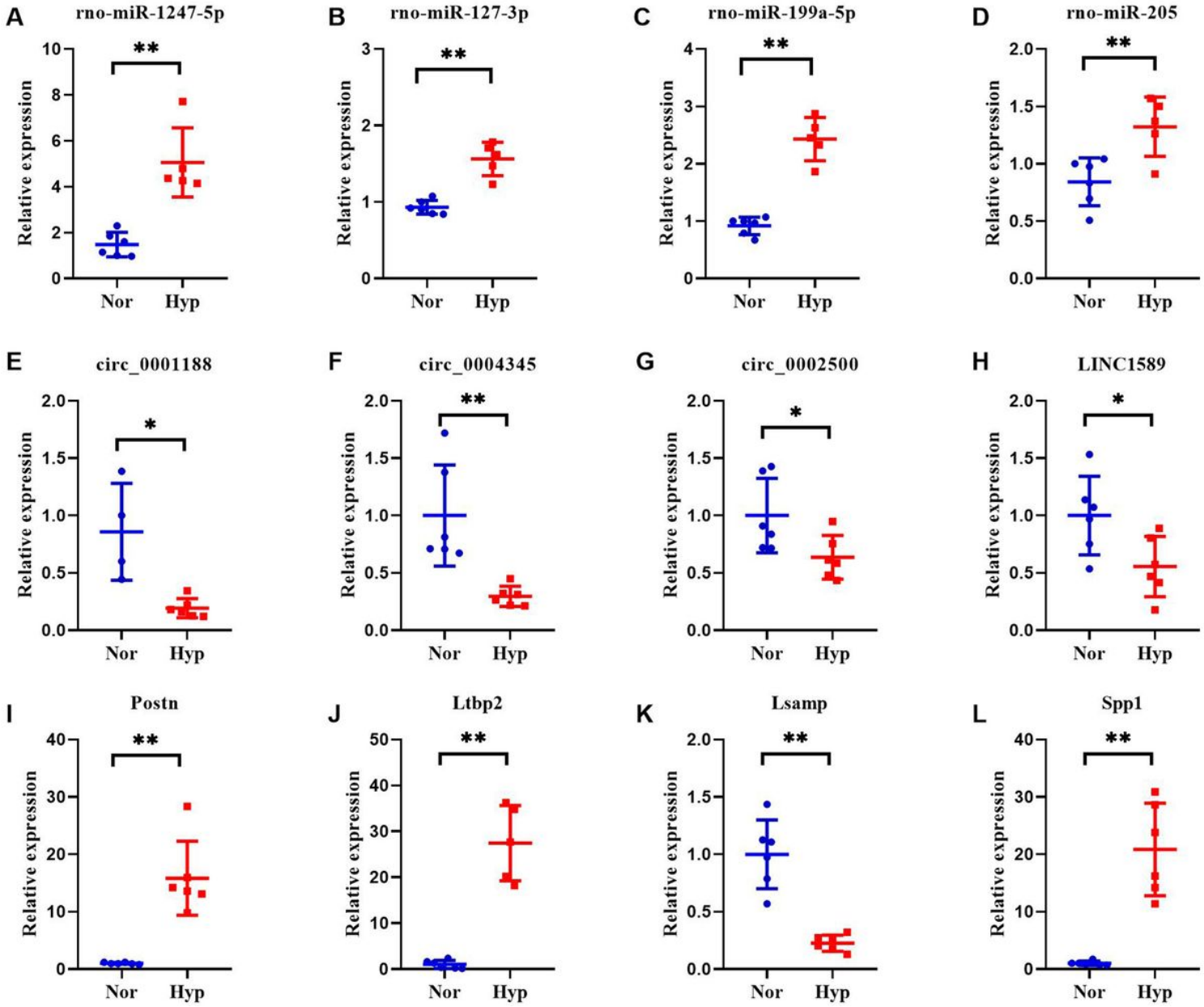

Figure 6

The expression profiles of selected DERNAs in ceRNA network. Expression level of rno-miR-1247-5p (A), rno-miR-127-3p (B), rno-miR-199a-5p (C), rno-miR-205 (D), circ_0001188 (E), circ_0004345 (F), circ_0002500 (G), LINC1589 (H), Postn (I), Ltbp2 (J), Lsamp (K) and Spp1 (L) in pulmonary arteries of both HPH and normal rats. Nor, normal control rats; Hyp, hypoxia-induced pulmonary hypertension (HPH) rats.

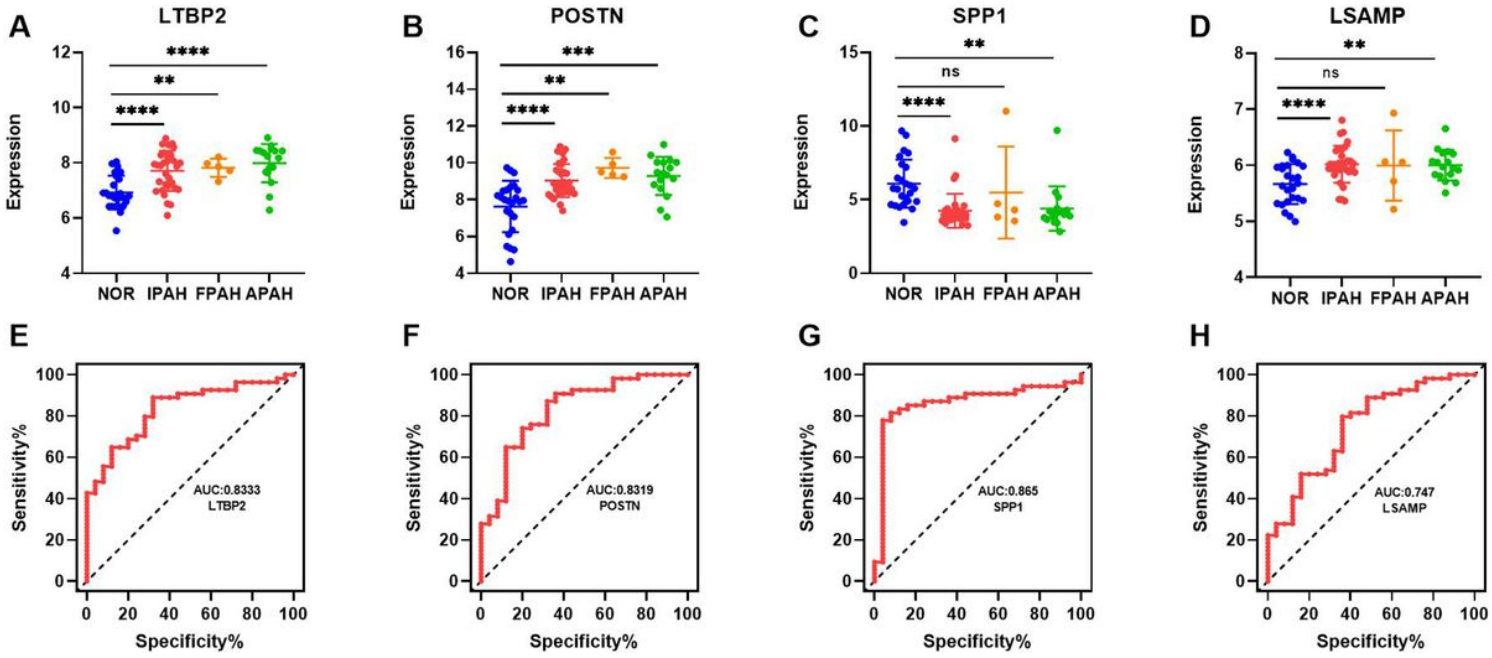

Figure 7

Evaluation of the diagnostic value of potential hub mRNAs in patients with pulmonary artery hypertension (PAH). Expression profiles of LTBP2 (A), POSTN (B), SPP1 (C) and LSAMP (D) in the lung tissues of PAH patients and normal individuals. NOR, normal individuals. IPAH, idiopathic PAH; HPAH, heritable PAH, APAH, associated PAH (connective tissue disease, congenital heart defects, anorexigen/stimulant drug use and so on). *p < 0.05, **p < 0.01, ***p < 0.001, and ****p < 0.0001. ROC curve analysis of potential diagnostic mRNAs. The AUC curve showed the effectiveness of LTBP2 (E), POSTN (F), SPP1(G) and LSAMP (H) for the detection of the occurrence of PAH.

Supplementary Files

This is a list of supplementary files associated with this preprint. Click to download.

- Additionalfile1.xlsx